Original Article

Identification of pulpitis at dental X-ray periapical radiography based on edge detection, texture description and artificial neural networks

Bernard Y. Tumbelaka, Fahmi Oscandar[1], Faisal Nur Baihaki, Suhardjo Sitam[1], Mandojo Rukmo[2]

Departments of Physics, Faculty of Mathematics and Natural Sciences, [1]Radiology Dentistry, Faculty of Dentistry, University of Padjadjaran, Jatinangor, [2]Conservative Dentistry, Faculty of Dentistry, University of Airlangga, Surabaya, Indonesia

Key words

Arti¿cial neural networks, dental X-ray, edge detection, image entropy, mean square error, periapical radiography, pulpitis, texture description

ABSTRACT

Objectives: The aim of the present research was to identify pulpitis through periapical radiography by applying edges as basis image features, the texture description and the arti¿cial neural networks (ANNs). **Materials and Methods:** Input image data records of 10 molar and 10 canine teeth were used. The clinical diagnosis of interest cases were represented as normal pulp, reversible and irreversible pulpitis, and necrotic pulp. The following image processing steps were done. First, the data records were converted digitally and preprocessed as its original image using the Gaussian Filter to obtain the best smoothed intensity distribution. Second, the local image differentiation was used to produce edge detector operators, e(x,y) as the image gradient; ∇f(x,y) providing useful information about the local intensity variations. Third, these results were analyzed by using the texture descriptors to obtain digitally the image entropy, H. The fourth step, all were characterized by the ANNs. **Results:** The edge detection carried important information about the object boundaries of pulpal health and pain conditions in the dental pulp signi¿cantly. The image entropy which was identi¿ed, the diagnostic term, was obtained from texture descriptors in the segmentation regions where the curves of pulp states tent convergence with the normal pulp line from 4.9014 to 4.6843 decreasing to the reversible and the irreversible pulpitis line include the nectrotic pulp line from 4.6812 to 4.5926 and then inputting to the ANNs analysis at the same of mean square error around 0.0003. **Conclusions:** Referred to these results, the correlation of the image entropy and the ANNs analysis could be linearly classi¿ed with the critical point of 4.6827. Finally, it could be concluded that the direct reading radiography is better to be digitized in order to provide us the best choice for diagnosis validation.

Address for correspondence:
Prof. Bernard Y. Tumbelaka,
Faculty of Mathematics and Natural Sciences, University of Padjadjaran, Jatinangor, Indonesia.
E-mail: btumbelaka@ymail.co

among all ages especially younger people due to several unhygienic factors like smoke, hormonal disturbance in woman, diabetes, stress, cancer, AIDS, genetic factors, insufficiently nutrients, and drugs.[4]

An attempt to find a new method in radiography that could identify this inflammation of tooth pulp in soft tissue is worth to try it. The pulp is the inner part of the tooth that consists of blood vessels, nerve endings, and connective tissues. The primary objective of pulp therapy is to maintain the integrity and health of the teeth and their supporting tissues. The indications are based on the clinical diagnosis of normal pulp, reversible pulpitis (pulp is capable of healing), symptomatic or asymptomatic irreversible pulpitis (vital inflamed pulp is incapable of healing) and nectrotic pulp or pulpless (pulp do not respond to vitality test).[5-8] It might be interesting to try to find these indications that could be obtained from radiographic evidence of periapical radiolucency to diagnose pulpitis. It was impossible to achieve an accurate diagnosis of the state of the pulp on the basis of clinical proof alone. The only accurate method is to do a histological examination.[9] Therefore, numerous classifications of pulp disease had only identified by a limited number of clinical diagnostic tests before effective dental treatment is performed. Therefore, our research interest was aimed to identify pulpitis in the regions of interest through periapical radiography by applying edges as basis image features, the texture description and the artificial neural networks (ANNs).

MATERIALS AND METHODS

Input image data of 10 molar and 10 canine teeth of periapical radiography of X-ray were used. The clinical diagnosis of interested cases was separated into four tooth conditions of pulpal diagnose states: normal pulp, reversible and irreversible pulpitis and necrotic pulp. The following image processing steps were separate the pulpitis. It could be also separated the infected line in two regions of interest as the reversible pulpitis and the irreversible pulpitis. The process used weight input generated that was always trained until reached the result of learning appropriate data same as identified. For the first training as compared variables let amount of database. Furthermore, these selected number of database input would be very influence the analysis results because the identification error would be able corrected if only if the weight input database were more added.

Experimental setup

These research works were arranged for the preprocessing and processing of the original image to obtain the best intensity distribution using Gaussian filter and to identify the tooth in the next step by the edge detection as the basic image features of the disinfected and infected tooth regions of image segmentation separately to find the deterministic processing [Figure 1]. When the non-deterministic cases were obtained, it was needed to apply the ANNS analysis.

Gaussian filter

It was needed to apply a very commonly used filter, which smoothly, reduces noise and gets small details. Equation[1] of a Gaussian function in two dimensions was the product of two of one-dimensional Gaussians, one in each dimension, $G_\sigma(x, y)$ as follows:

$$G_\sigma(X,Y)=\frac{1}{2\pi\sigma^2}\exp\frac{-X^2+Y^2}{2\sigma^2} \qquad [1]$$

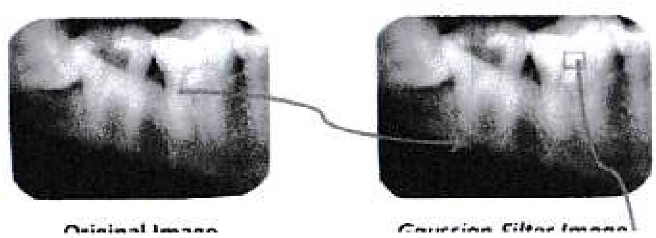

$$MSE = \frac{1}{N}\sum_{i=1}(T_i - O_i)^2 \quad [12]$$

where: N – number of database, i = 1,2,3., N, T – final data output, O - true data output.

RESULTS

Results are summarized in Table 1 and Figures 2-6. Ten tooth radiographs were used according to the ROI (region of interest) of 10 cropped samples for normal pulp, reversible and irreversible pulpitis, and necrotic pulp. There could be several results described as follow.

First, the edge detection carried important information about the object boundaries as normal pulp, reversible and irreversible pulpitis, and necrotic pulp significantly which could be valuable for the pulp interpretation as shown in Figures 2a and b.

Second, as shown in Figures 3 and 4 and Table 1, first by using mean analysis was obtained directly for normal pulp of region 1 (171.3669) to region 8 (171.5720), and normal pulp to pulptis line separated by reversible of region 8 to region 12 (186.7028), irreversible of region 12 to region 17 (185.5005). Second, variance analysis was also used for normal pulp of region 1 (62.9592) to region 8 (54.8623), and normal pulp to pulpitis line separated by reversible of region 8 to 12 (55.2579), irreversible of region 12 to 17 (46.5700). In Figure 5, by using image entropy obtained from texture descriptors by mean and variance analysis[15] as deterministic and random curve. The curves of normal pulp and pulpitis regions were figured convergence with normal pulp line from 4.9014 to 4.6843 decreased to pulpitis line from 4.6812 to 4.5926 with MSE around 0.0003, as shown in Figure 6.

Table 1: The relationship between variance and mean regions for normal pulp, reversible and irreversible pulpitis, necrotic pulp regions

	Normal tooth		Pulpitis		Dead tooth
	Normal pulp	Reversible	Reversible	Irreversible	Necrotic pulp
	1 to 8	8 to 11	11 to 12	12 to 17	18 to 20
Variance	62.9592 to 54.8623	54.8623 to 55.2579		55.2579 to 46.5700	46.5700 to 38.4427
Mean	171.3669 to 171.572	171.572 to 186.7028		186.7028 to 185.5005	185.5005 to 183.4223
Image Entropi	4.9014 to 4.6843			4.6812 to 4.5926	

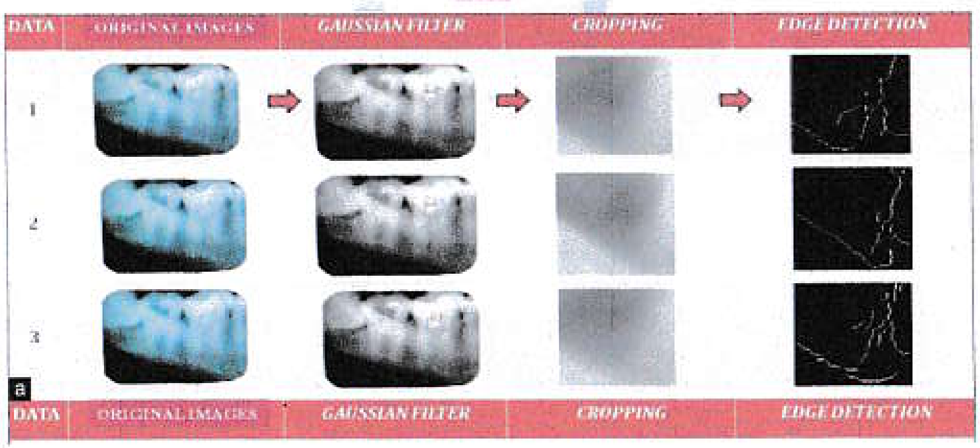

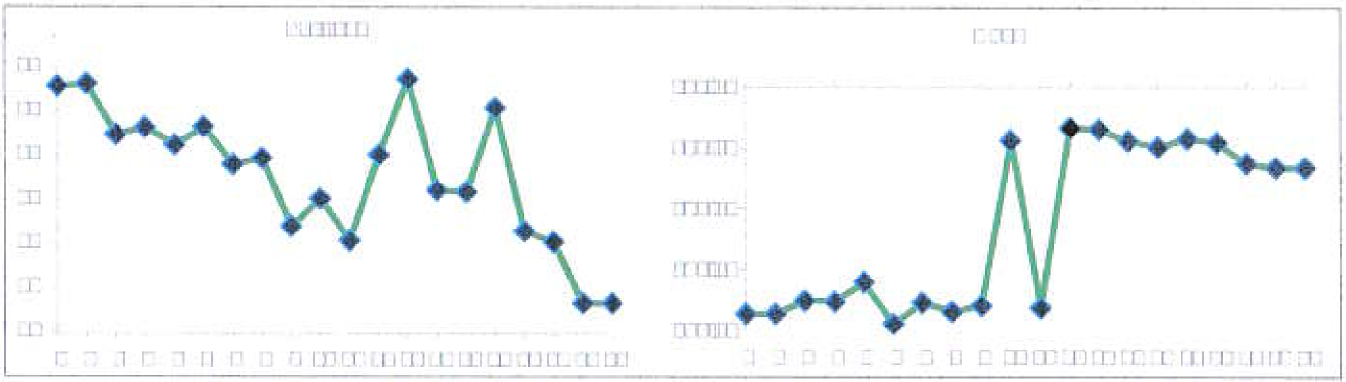

Figure 3: Curves of variance and mean analysis for normal pulp, reversible, irreversible, necrotic

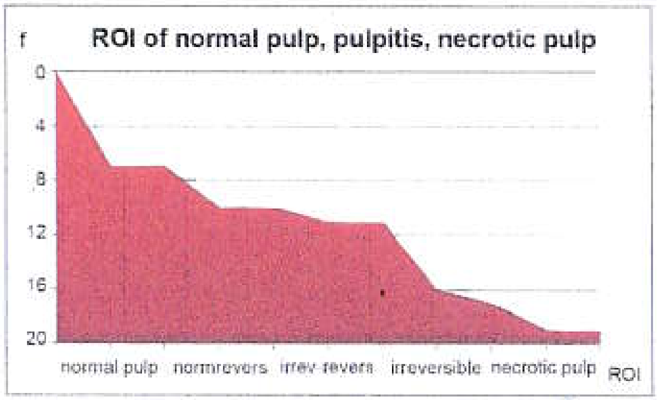

Figure 4: Correlation between ROI of f and ROI of disinfected and infected by pulpitis based mean and variance

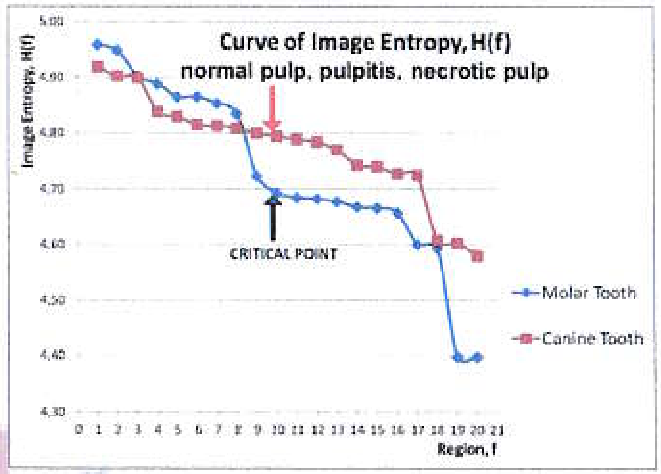

Figure 5: Curve of image entropy of normal pulp, reversible and irreversible pulpitis, and necrotic pulp

The results could be inputting and expanding our observation figured convergence at the normal pulp and pulpitis regions with normal pulp line decreased to pulpitis line with the critical point by the texture description and the ANNs analysis at the same of MSE around 0.0003. Figure 6 gave the nonlinearity of the MSE curve representing the accuracy of final output over the true output during the training. Pulpitis identification was done through ANN analysis, where accuracy was the percentage of number of true classified compared to all final result classified. For observation that resulted with the reaching true

reversible pulpitis (4.6827 to 4.6565) and the irreversible pulpitis (4.6565 to 4.3973).

DISCUSSION

Even though the periapical radiographic film was of high quality, there might be more important information that could not be directly detected in regard to the pulp disease states. The present research involved to reduce the diagnosis suspect and to gain accurate diagnosis that

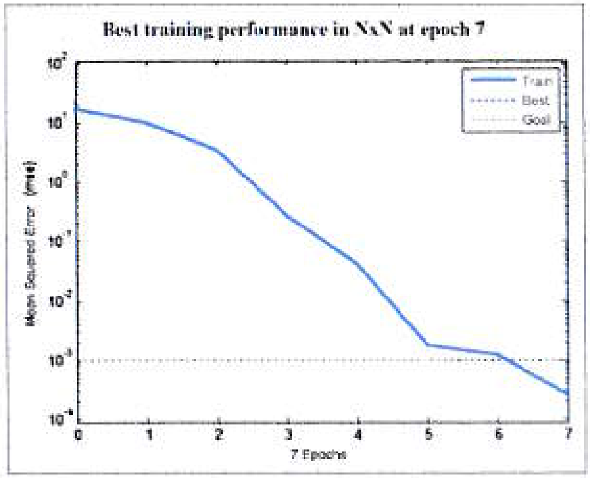

Figure 6: Diagnose the best training performance in 32 × 32 iterated at epoch 7 of data testing simulation using by ANNs analysis

The principles for diagnosis of the condition of the dental pulp are no different from those applied to the management of other disease conditions. One of the essential methods is radiographic examination which is an important complement to the clinical examination. It provides information about the presence and severity of caries, deep restorations in relation to the dental pulp as well as root fractures and periapical changes.

Our research started with the dental image quality problem that was usually degraded because of its mechanical, optical and electronic noises from its medical tools were utilized. A Gaussian filter smoothes an image by calculating weighted averages in a filter box.[22] Therefore, we had to perform the image pre-processing using a Gaussian filter approximated to its original image as the best intensity distribution that analyzes its image identification and feature parameters linked with the features on object represented in the image. The image features of edge detection represented and correlated with means and variances identifying the state of normal pulp, pulpitis and necrotic pulp as a deterministic solution. These with the critical point by the texture description and the ANNs analysis. It might be interesting to develop a learning process from number of database changed for user's needs with high flexibility and standardization.

Although there were always some exceptions, the different symptoms usually detect that a patient presents with the pulpal diseases. Image entropy could be expanded to multivariate function where the pulp pain in higher sensitivity degenerated to the state of dead pulpal tissue. This will be our new and future research goal.

CONCLUSIONS

The correlation of the image entropy and the ANNs analysis could be linearly classified with the critical point of 4.6827. Finally, it could be concluded that the direct reading radiography is better to be digitized in order to provide us the best choice for diagnosis validation.

ACKNOWLEDGMENTS

We acknowledge the great collaboration between Faculty of Dentistry and Faculty of Mathematics and Natural Sciences of University of Padjadjaran and Faculty of Dentistry, University of Airlangga, Indonesia.

REFERENCES

1. Mulyani D, McIntyre J. Caries inhibitory effect of fluoridated sugar in a trial in Indonesia. Aust Dent J 2002;47:314-20.
2. Gutmann JL, Baumgartner JC, Gluskin AH, Hartwell GR, Walton RE. Identify and define all diagnostic terms for Periapical/Periradicular health and disease states. J Endod 2009;35:1658-74.
3. Dos Santos Guimarães C, Sampaio GC, Barros de Almeida E, Silva LB, Mourato AP, Alves DF. Influence of Apical Foramen Cleaning on Periapical Lesion Repair. Rev Fac Odontol Porto Alegre 2011;52:45-7.
4. Mayo Clinic. Oral health: A window to your overall health. Mayo Foundation for Medical Education and Research. Available from: http://www.mayoclinic.org/dental/[Last accessed on

where: x is the distance from the origin in the horizontal axis, y is the distance from the origin in the vertical axis, σ is the standard deviation of the Gaussian distribution.

It was also needed to use the discrete convolution of equation [2] as follows:

$$f * g = \sum_i f_i \, g_{x-i} \qquad [2]$$

where: f is the image function, g is the Gaussian function

When it was applied to the edge detection, it might be a derivative of a noisy signal that could cause more noise. Therefore, it was needed to apply the Gaussian filter before taking a smoothed derivative. The differentiation and convolution of equation [3] both linear operators where they commuted together as

$$\frac{d}{dx}(f * g) = \frac{df}{dx} * g = f * \frac{dg}{dx} \qquad [3]$$

Edge detection

Image edges were the form of local variations of image intensity that can produce local image differentiation techniques defined as edge detector operators, the image gradient, ∇f(x,y) could be written as equation [4]:

$$\nabla f(x,y) = [f_x \; f_y]^T, \qquad [4]$$

where: $f_x = \partial f/\partial x$ and $f_y = \partial f/\partial xy$ are the gradient operators, T is the matrix transpose

This gave useful information about local intensity variations. The edge detector, e(x,y) was obtained as the magnitude of f (x, y) that can be written as equation [5]:

$$e(X,Y) = \sqrt{f_x^2(X,Y) + f_y^2(X,Y)} \qquad [5]$$

The sum of the absolute values of partial derivatives f

Texture descriptors

Mostly, an image characteristic depend on its texture used in the region segmentation. There were several important simple texture descriptors such as the image histogram $p_f(f_k)$, the arithmetic mean, μ in equation [8] and the variance of the standard deviation square, σ^2 in equation [9] and the image entropy, H in equation [10] as a scalar value representing the entropy of gray scale image, f_k having B pixels are given by:

$$\text{Mean} \quad : \mu = \sum_{k=1}^{B} f_k p_f(f_k) \qquad [8]$$

$$\text{Variance} : \sigma^2 = \sum_{k=1}^{B} (f_k - \mu)^2 p_f(f_k) \qquad [9]$$

$$\text{Image Entropy: } H(B) = -\sum_{k=1}^{B} p_f(f_k) \ln p_f(f_k) \qquad [10]$$

where: $p_f(f_k)$ – the image histogram, f_k – is the various image intensity levels, $0 \le f \le 2^B$, k – is the pixel location, k = 1, 2,...., B, B – gray scale unit, 2 bits, 4 bits,....

Usually, entropy was a statistical measure of randomness that can be used to characterize the texture of the input image histogram. The image histogram was calculated within an image region, f.

The relation between the average codeword length, L(f), and the image entropy was very close that could be written as equation [11]:

$$H(B) \le L(f) \le H(B) + 1 \qquad [11]$$

Entropy of the gray scale image contained of thousand bits of information, representation of intensity. Entropy converted any class other than logical to unit 8 for the histogram count calculation so that the pixel values were discrete and directly correspond to a bin value. Using these texture descriptors, it was deterministic analysis that could refuse several descriptor cause

histological findings in the pulp. Oral Surg Oral Med Oral Pathol 1963;16:969-77.
10. Mathematica, Gaussian Filter function. Available from: http://www.reference.wolfram.com/mathematica/ref/GaussianFilter.htm. [Last accessed on 2012].
11. Fisher R, Perkins S, Walker A, Wolfart E. Spatial Filters: Laplacian of Gaussian. Available from: http://www.homepages.inf.ed.ac.uk/rbf/HIPR2/log.htm [Last accessed on 2003].
12. Conners RW, Harlow CA. A Theoretical comparison of texture algorithms. IEEE Trans Pattern Anal Mach Intell 1980;2:204-22.
13. Pitas I. Digital image processing algorithms. United States: Prentice-Hall, Inc. Upper Saddle River, NJ, USA. 1993
14. Gonzalez RC, Woods RE, Eddins SL. Digital image processing using Matlab. NJ. Chap 11. United States: Prentice Hall; 2003.
15. Matlab products. Available from: http://www.mathworks.com/matlabcentral/fileexchange/26694-gray-level-run-length-matrix/content/GLRLM.[Last accessed on 2012 Dec 12].
16. Nair MK, Nair UP. Digital and Advanced Imaging in Endodontics: A Review. J Endod 2007;33:1-6.
17. Abella F, Patel S, Duran-Sindreu F, Mercadé M, Bueno R, Roig M. An evaluation of the periapical status of teeth with necrotic pulps using periapical radiography and cone-beam computed tomography. Int Endod J 2014;47:387-96.
18. Nance R, Tyndall D, Levin LG, Trope M. Identification of root canals in molars by tuned-aperture computed tomography. Int Endod J 2000;33:392-6.
19. Lozano A, Forner L, Llena C. In vitro comparison of root-canal measurements with conventional and digital radiology. Int Endod J 2002;35:542-50.
20. Jung M, Lommel D, Klimek J. The imaging of root canal obturation using micro-CT. Int Endod J 2005;38:617-26.
21. Yoshioka T, Kobayashi C, Suda H, Sasaki T. An observation of the healing process of periapical lesions by digital subtraction radiography. J Endod 2002;28:589-91.
22. Liu Ce, Szeliski R, Kang SB, Zitnick CL, Freeman WT. Automatic Estimation and Removal of Noise from a Single Image. IEEE Trans Pattern Anal Mach Intell 2008;30:299-314.
23. McClanahan SB, Johnson JD, Blundell RE Jr. Pulpal and periradicular diagnostic terminology. Naval Postgrad Dental School National Naval Dental Center, Bethesda, Maryland. Clinical Update. Vol. 24, No. 1 January 2002.
24. American Academy of Pediatric Dentistry (AAPD). Guideline on Pulp Therapy for Primary and Immature Permanent Teeth. Reference Manual. IV 34. No 6. 12/13. 2009. p. 222-9.

How to cite this article: Tumbelaka BY, Oscandar F, Baihaki FN, Sitam S, Rukmo M. Identi¿cation of pulpitis at dental X-ray periapical radiography based on edge detection, texture description and arti¿cial neural networks. Saudi Endod J 2014;4:115-21.

Source of Support: Nil. ConÀict of Interest: None declared.